Paper III

Principles of MIR, Multivariate Image Regression - I:

regression typology and representative application studies

by

Thorbjørn T. Lied & Kim H. Esbensen

	Corresponding Author	Senior Author
Name	Thorbjørn Tønnesen Lied	Kim H. Esbensen
Phone	+47 35 57 51 53	+47 35 57 51 50
e-mail	thorbjorn@lied.no	Kim.Esbensen@hit.no
Company	Telemark University College (HIT) Department of Technology (TF) Applied Chemometrics Research Group (ACRG)	
Address	Kjølnes Ring 56 N-3914 Porsgrunn Norway	
Fax	+47 53 57 52 50	

CONTENTS

ii

Principles of MIR, Multivariate Image Regression - I: regression typology and representative application studies

ABSTRACT

We present an introduction to MIR: Multivariate Image Regression with a selection of illustrative application studies. Generalisation from 2-way multivariate calibration to the 3-way regimen leads to - at least - three alternative *image regression cases* depending on the nature of the available Y-data: IPLS-$Y_{discrim}$; IPLS-Y_{grid} ; IPLS-Y_{total} . A systematic *image regression typology* is briefly introduced.

We here present the core of the principles of *applied* MIR: Two major MIR application studies are worked through, a food mass product industrial inspection study (IPLS-$Y_{discrim}$) and a food product (fruit) storage stability image analytical monitoring (IPLS-Y_{grid}). These exemplifications are presented as *archetypes*, representing a much wider range of potential industrial/technological application areas.

The present paper represents one major element of our work towards establishing a complete, stand-alone facility for MIR (Multivariate Image Regression); the second paper in this series deals with the development, implementation and extensive exemplifications of a complementary cross-validation facility.

KEYWORDS: multivariate image regression; MIR; multivariate image analysis; MIA; multivariate image texture analysis; MIX; 2-D images; 3-D image arrays; *image regression cases*; applications

1.0 INTRODUCTION

The introduction of the Multivariate Image Analysis (MIA) concept in cheometrics was not longer ago than Esbensen & Geladi (1989) [1]. In the intervening 10+ years the development of MIA has been relatively slow, but would appear to begin to take to speed more recently - the entire field was summarised in the comprehensive textbook by Geladi & Grahn [2]. Much of the theoretical background for Multivariate Image Regression (MIR) necessitates a thorough understanding of the principles and methods in MIA, which we shall here assume known. It is especially important that the concept of the *multivariate image* is well understood.

Because regression calculations on the extensive amount of data in multivariate images easily can be a technical challenge (growing quadratically with the number of variables, or channels), some important recent evolutions have made it more feasible in the last few years. The continuously developing technical improvements in computer hardware efficiency is of course a major contributor, but especially the KERNEL PLS algorithm introduced by Lindgren et.al. in 1993 [3] has dramatically speeded up the present type of calculations, as was outlined in detail in [5].

Despite of this, few studies has yet shown the true potential of MIR as a tool for predicting quantitative features in multivariate image data. Hopefully, this condition will be improved by the current paper.

1.1 Concepts

Several concepts are used in this paper, some of which may be relatively unfamiliar. A brief introduction of these is given to help the reading of the article.

1.1.1 Multivariate Image (MI): The MI is a digital image of *one* scene, consisting of *many* variables (channels), e.g. colour bands, channels. At the outset the simplest situation is the one in which each image *pixel* is treated as an *object*, which requires rigid consistency in scene lay-out for all variables. An object in a given scene position in one variable must be found in the same scene position in all other channels; for regression cases also in the Y-image. MI's are usually presented as a 3-D matrix, but because the two object-ways can be treated as one way, the MI may also be reorganized into a 2-D-matrix prior to modelling, and 2-way methods can be applied [2] by way of the so-called *unfolding* operator.

1.1.2 MIR: Multivariate Image Regression [2, 4] builds regression models between the multivariate X-image and the (uni-/multi-)variate Y-image. MIR is here performed

using KERNEL-PLS [3, 5] on reorganized Multivariate Images, i.e. each variable is reorganised into a (very long) object vector. In this basic unfolded form, MIR uses only the variable-signatures, i.e. the spectral information the analysis and only indirectly makes use of the spatial information analogous to MIA [1, 2]. But even though MIR technically uses 2-way analytical methods, there is an enormous visualisation potential in image data which is also used fully in MIR. Displaying results not only in score space, but also in the so-called *backfolded* image space, enhances the insight in the data structure and the models developed. Applying colour coding to score plots, MIA, or by combining three score images in one composite ("R/G/B") colour image, it is often possible to capture comprehensive model presentations of great interpretation value etc..

1.1.3 MIX: Multivariate Image teXture analysis. MIX is an extended MIA-MIR approach which includes spatial, especially textural, information in the analysis. In cases where spatial information is important, this can be included in the MIR-model by e.g. adding derived textural variables calculated from the original variables [6-8]. Sometimes enhancing details using e.g. edge-detectors is favourable, in other cases the opposite (smoothing details) might be required etc. Also, *combining* textural filters might often give very useful results. MIX has the potential for explosive data growth, thus powerful means for variable selection are required. We do not treat the MIX aspects in any depth in the present work however.

1.1.4 Regression typology

Perhaps surprisingly, going from the 2-way realm in which the concepts of multivariate calibration is well-known - and need no further presentation here - there is a corresponding three-fold multitude of analogous but in principle different image *regression modes*, Figure 1.

1.1.4.1 IPLS-Y$_{discrim}$: The Yes/No classificator/discriminator. In every position in the Y-image, a pixel is either 1 (one) if it is part of a current class, otherwise 0 (zero). The approach is suitable for classifying one class among (many) others. Used as a pre-processor, this method can easily be taught how to pick out desired classes. This case is also easily extended to cover several classes, by using several one-class Y-discrim masks, Figure 1.

1.1.4.2 IPLS-Y$_{grid}$: If every Y-condition is not available in one image, several images can be juxtaposed in a compound, so-called *gridded* image. This way the total experimental design can be represented in one image, i.e. one model. Extensive

illustration of IPLS-Y_{grid} is given in this work. In some cases, especially when predicting an overall value for each sub-image in the grid, the corresponding Y-image will have a constant value within each sub-image. When this appears, some kind of smoothing of each sub-image in X will usually be useful, i.e. reducing non-classification related variations in X.

1.1.4.3 IPLS-Y_{total}: When the entire experimental design is covered in one frame, merging images together, as in the IPLS-Y_{grid} is not required. In these cases, each pixel in X also has a separate, unique value in the Y-image. Typical examples come from e.g. remote sensing. Because most of the still limited MIR-literature explicitly discusses this kind of data, and because it is merely a special, extreme case of the Y_{grid}, it will not be treated further in this paper
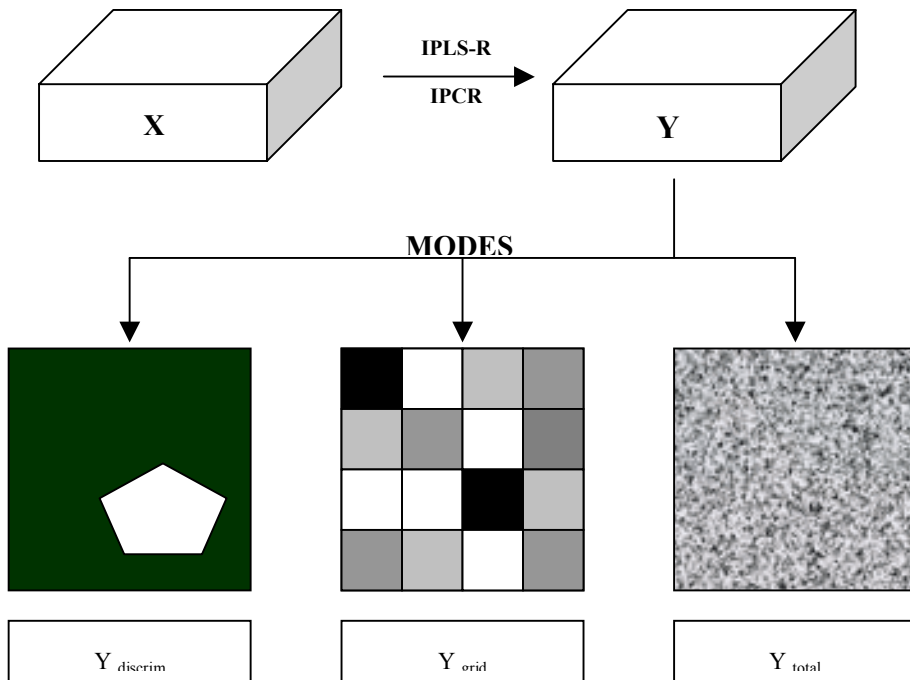

Figure 1. The three different MIR modes, $Y_{discrim}$, Y_{grid} and Y_{total}.

1.2 Software

All calculations in this paper are performed using a self-developed program, described in Lied, Geladi & Esbensen [5]. The software is available for Microsoft Windows ® (9X NT 4+5) and is written in National Instruments' LabVIEW v. 5.1. Both MIA and

MIR is implemented; for MIR regression calculations, KERNEL-PLS [3] is used exclusively. [1]

2.0 APPLICATIONS

Below the terminology IPLS (Image PLS) is used throughout, but it is evident that PCR *may* also be used alternatively should one so desire, albeit with the well-known distinctions regarding PCR vs. PLS [9-10] etc. Here PLS is employed exclusively because of its well-known chemometric advantages [9-14]. In both major examples below, data are mean centred and scaled to uniform standard deviation. All variables thus have equal variance weights, making the Kernel-PLS decompositions pertain to *correlations*.

2.1 IPLS-Y$_{discrim}$: Discrimination Prediction.

Motivation: A *pilot study* of image analytical *industrial inspection* of a mass production food article, Swedish crispbread ("knäckebrød") is presented. This item, by nature of its mass consumption status, is produced in very large quantities in industrial bakeries in many countries. Output from the industrial ovens are necessarily way outside *complete* human inspection capabilities, for which reason an automated, industrial image analytical system would be of considerable interest. This in turn could form the basis for a truly 100% inspection system.

In our restricted pilot study involving some 10 pieces of crispbread, parallel representative oven outputs are available, 5 with an "accepted" status and 5 with three types of representative faults, typically encountered in the industrial production situation. Figure 2 shows these three faults together with examples of the directly acceptable product ("normal"). Technical details regarding this image is found in table 1.

---

[1] When developing this prototype, serious efforts were made to enhance the flexibility and user interaction facilities. For large datasets, 10 M pixels or above, calculations starts to become slow however. Development of a professional system is now under way. Contact the corresponding author for instructions on how to download the freeware *prototype*.

Table 1. Technical Details of the crispbread case

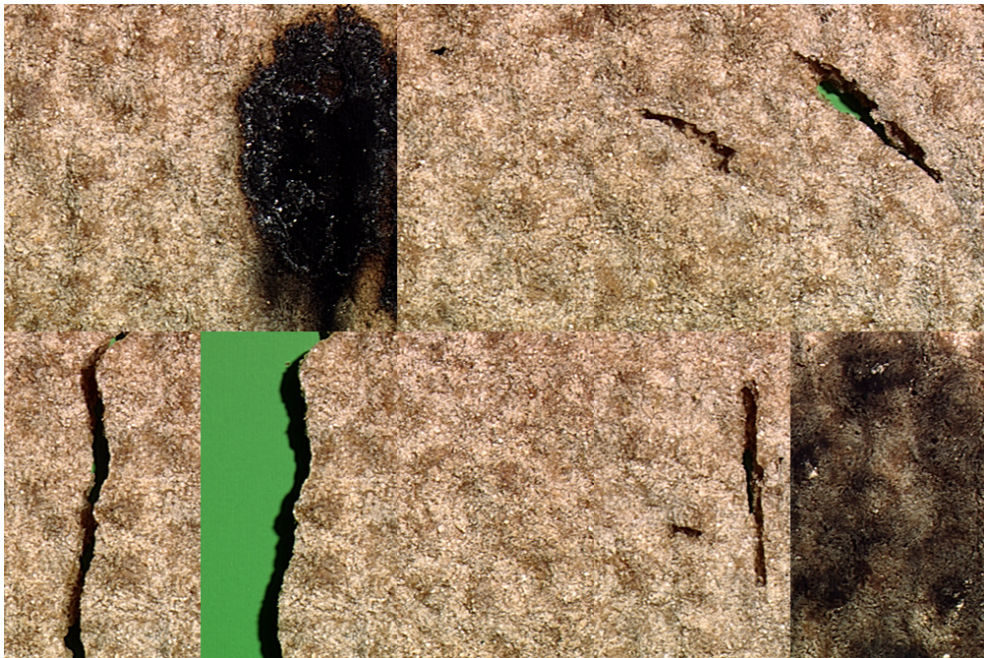| Image Capture	Camera	Lens	Focal Length
	JVC 3CCD KYF-50	Micro Nikkor AF	105mm
Measures	With (pixels)	Height (pixels)	# Variables
Total Image	1000	666	4
Sub Images	200	333	4
Spectral Variables	Colour	Wavelength	Bandwidth
1	RED	N/A	N/A
2	GREEN	N/A	N/A
3	BLUE	N/A	N/A
Textural Variables	Filter	Window Size & Passes	Applied to
1	Variance		

Figure 2. "Normal" and "flawed" Scandinavian crispbread ("knekkebrød"). Three representative types of flaws are displayed; broken, perforated and burnt cases.

Figure 3 shows standard MIA score plot set-ups for the crispbread case (figure 2) [1, 2].

In the interest of the wider application horizon for this specific IPLS-$Y_{discrim}$ regression example, a more *general* IPLS-$Y_{discrim}$ regression case will be set up. This is done by using a *Y-image mask* of the areas of interest in the image which are recognised as "rejects", i.e. areas which are underlain by those parts of the Y-image which depicts flaws of the various type. Figure 4 shows this "flaw"-mask.
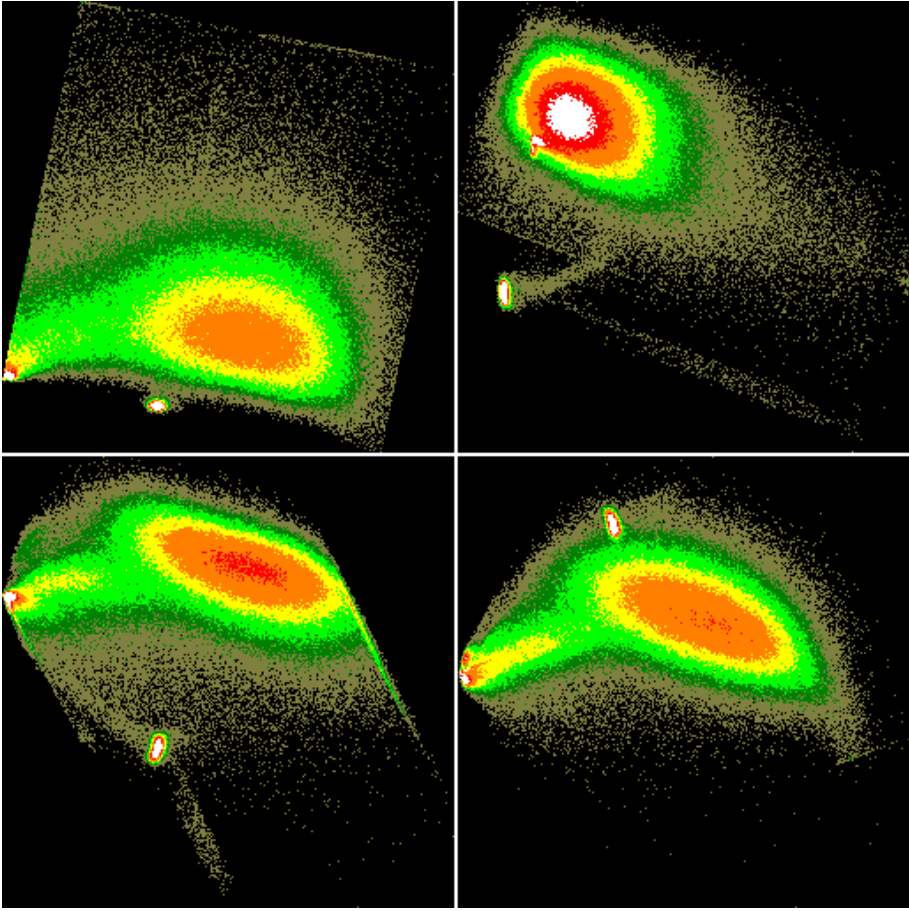
Figure 3. MIA standard score-plot for the crispbread case in figure 2.

Figure 4. Y-image mask of (0/1) discrimination areas. Note that by using a relevant background discrimination feature, it is possible to zoom in only on the true flaws present in the gridded calibration imagery, which have been designated white here.
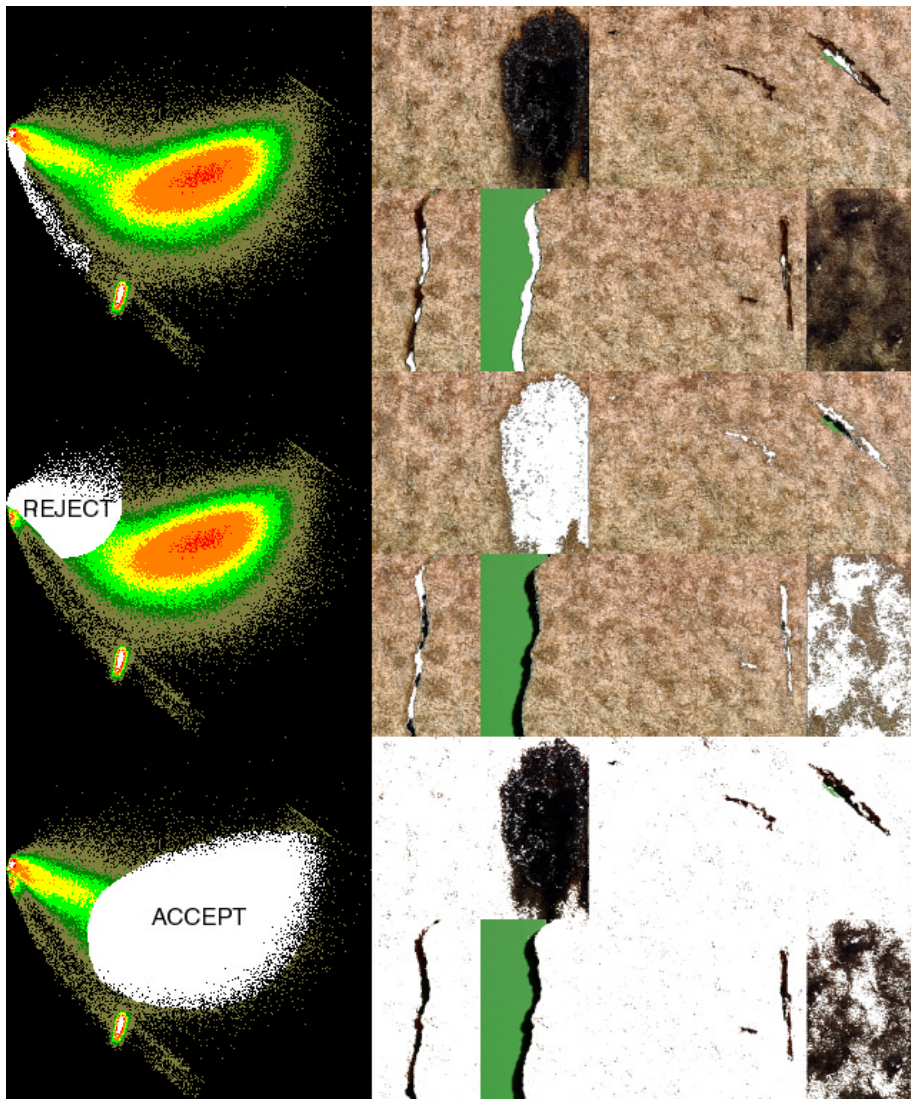
Figure 5. IPLS-Y$_{discrim}$ t1-t4 score plots showing all three resolved classes in the crispbread case: broken/perforated (top panel); burnt (middle) and "accepted" (lower). Note complete discrimination. Also comp. with similar t1-t2 scoreplot from the MIA-solution

Figure 5 has been designed to bring forth the full potential of the IPLS-Y$_{discrim}$-case, showing (in standard MIA-style) the corresponding t1-t4 score plots *versus* the original (raw) image domain layouts of three fault classes present in the fully background-discriminated crispbread case: shadow (top); burnt (middle) and "accepted" (bottom). It is gratifying to observe *complete discrimination* between all relevant classes, i.e. all three types of rejects/accepted and the background as well. This

successful discrimination points directly to the desired use of image-based *prediction* of all these types crispbread. This pilot study, while extremely simple, allows full conceptual delineation of a complete automated image analysis system, by way of the relevant PLS-prediction facility, Figure 7.

Figure 6. Calibrated X-variance (top) and Y-variance (middle) and validated PRESS (low) for the crispbread case in figure 2.

Incidentally, observe that in this particular case, there would appear to be very little "tilting" of the IPLS-solutions relative to the corresponding simpler PCA-solutions (MIA), contrary to many other two-way experiences [4-5, 15-16]. In the present case this reflects a rather direct correspondence of the X-block data structure with the Y-structure(s), i.e. the information gathered in the image analytical X-decription "happens" to be directly correlated to the guiding Y-discrimination dummy variable; see also below however.

Figure 7. Predicted Ŷ-image using 1 (one) component. Note how the model distinguishes clearly between faults/non faults.

While figures 4-6 gives the statistical facts in this case, figure 7 shows the actual predicted image in scene space using one component. This figure demonstrates that the model is excellent for predicting all the relevant types of faults. This result is, needless to say, of a much larger generalisation potential than the specific crispbread example chosen. The illustration in fact has merit as an *archetype* for IPLS-$Y_{discrim}$ multivariate image regression.

MIX-aside: In this example a variance filter (table 1) has in fact also been applied to extract local textural variations in the X-image. While the background is flat, the crispbread has a very distinct, regular texture. The variance filter, which returns the local variance in a small window in every position in the image, will thus greatly help to *distinguish* crispbread from background as well as textureless burnt parts, assisting

the spectral information in the classification. The effect of this filter addition is visualized in figure 8 which shows the *loading weights*(w) for this example. From this figure, it can also be seen that X2 and X3 (Green and Blue) contains mostly the same information, indicating that one of them could be left out in later calibrations etc.
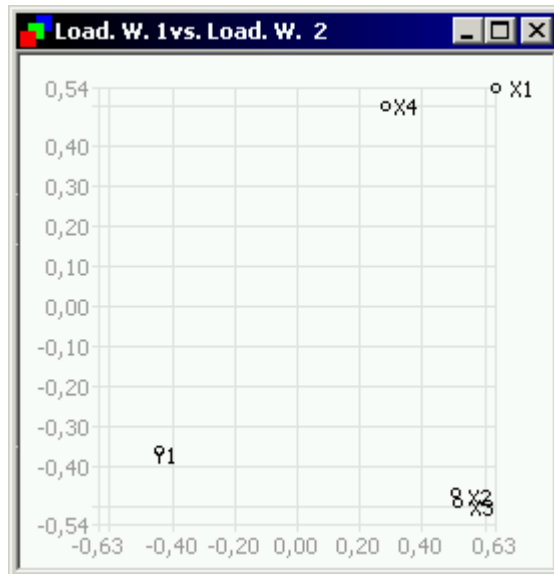

Figure 8. Loading weights 1 vs. loading weights 2 for the crispbread case. Note X-variables 2 (green) and 3 (blue) which seem redundant.

Note how judicious use of a *relevant background* (colour, texture) is essential to bring about the successful discriminations in this case. As in all image analysis applications *illumination* and *colouring* (not treated here) is often of equal importance compared to the data analysis proper etc.

2.2 IPLS-Y$_{grid}$: Monitoring and estimating storage time for fruit (bananas).

Motivation: The objective of this application example is to monitor storage stability by a series of (multi-temporal) images of the same fruit(s), with great efforts to keep all storage and imaging parameters *constant*, the only variable being time elapsed since storage start. Successful monitoring will allow for quantitative storage deterioration prediction directly from the captured multivariate X-images [5].

In this context, the calibration-parameter "storage time" shall be represented by juxtaposed part-images, making up a complete, so-called *gridded*, multivariate image, hence the suggested name for this second image regression mode: IPLS-Y$_{grid}$. This

example also serves as an *archetype* not only of multi-temporal studies but also of analogous objectives, conf. below.

Figure 9 shows the compound, gridded multivariate X-image of a deteriorating banana, for which the storage times involved are (from upper left to lower right): 1/2/3/6; 7/8/9/10; 13/14/15/20 days respectively. This gridded layout is necessary in order that all storage times can be *analysed together* by MIA or MIR. It is emphasized that it is the *objective* of the image analysis (in this case: storage stability monitoring) which *dictates* that the individual grids represent a succession of different storage times. For other image regression cases, these individual grid cells will often represent different, typical "object-like" categorical entities to be similarly *compared*, e.g. a series of different meats to be characterised, as was the case with Wold et al. [15] (in fact also predicting a storage-related parameter, "harshness"), Geladi and Grahn [2] a.o.

Table 2. Technical Details of banana example

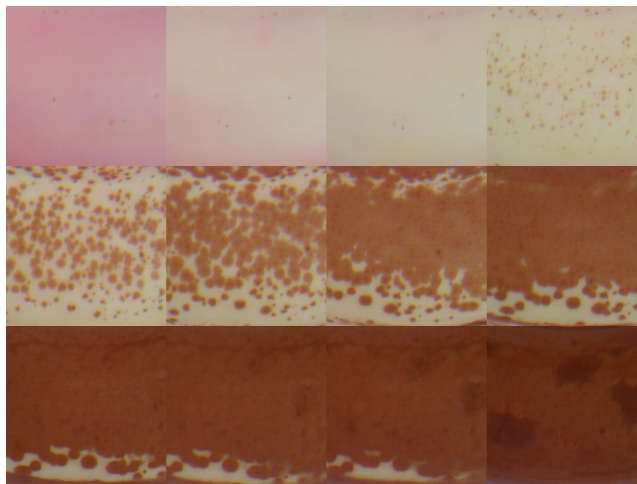| Image Capture	Camera	Lens	Focal Length
	SILVACAM	**Fujinon**	**120 mm**
Measures	**With (pixels)**	**Height (pixels)**	**# Variables**
Total Image	800	600	3
Sub Images	200	200	3
Spectral Variables	**Colour**	**Wavelength**	**Bandwidth**
1	NIR	760 - 900 nm	
2	Red	580 – 680 nm	
3	Green	490 - 580 nm	

Figure 9. Storage time aging of representative fruit (banana) in the interval 1-20 days.

In figure 10, which shows the particular *Y-image*, the *array* of grid cells forms the basis for an IPLS1. Observe how the deterioration process interval of 1-20 days has been *mapped* into an image analytical appropriate grey-level interval, spanning 0-255. Again it is the Y-image mask which makes the regression problem immediately appreciable. In one sense, as soon as the multivariate X-image has been defined, it is the Y-image which sets up the entire MIR.

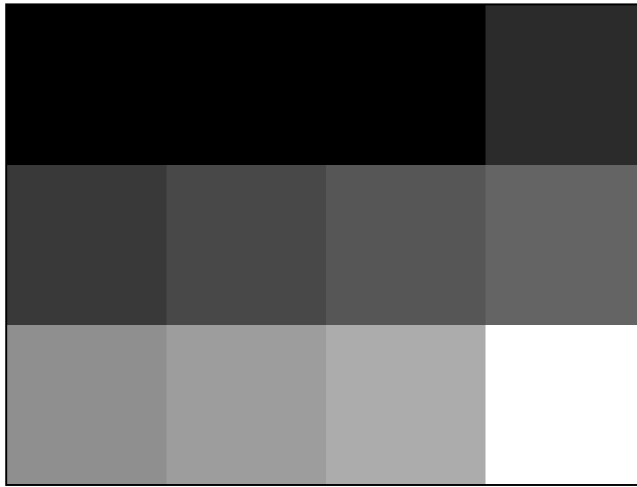*Figure 10. IPLS-Y_{grid} Y-image, delineating the problem-dependent Y-levels for the banana deteriorating process. Figure 10 (Y-image) corresponds to figure 9 (X-block).*

Figure 11 performs an identical role as figure 5, encompassing the essentials of the IPLS-analysis. In the t1-t2 score plot (upper left panel) one may appreciate, in full detail, the *trace* of the fruit deterioration process. [2] We have illustrated two representative *process stages* along this trace, an intermediate stage and the penultimate sad, almost totally rotten end of the banana development (upper right and lower left panel respectively). With reference to MIA [1, 2, 17] the scene-space back-

---

[2] We have elsewhere worked out a complete image analysis strategy, which - while originally presented as related to MIA - also applies to the *analogous* t-t- score plots derived by an IPLS-solution [17]. As but an example we there followed another biological process, albeit of considerable greater complexity, i.e. a forest clearing *regrowth* process, using geomorphological analogies in order to characterise MIA score plots. From this review [17] a range of interpretation guidelines for t-t score plots were developed, all of which may also be applied to the present PLS-solutions. Observe that a slightly different modus operandi applies to the t-u plots [18]. These subtle differences will be addressed in several sequel papers on a comprehensive MIR strategy, which are in the works.

projections of these two classes are self-explanatory in figure 11, especially when compared with figure 9. Fig. 11 shows how it is possible to delineate the *entire* deteriorating process in the X-space because the *entire* storage time *calibration span* has been compounded in the one (X,Y)-image.

For IPLS solutions the t-u score plot allows valuable, indeed critical insight into the *effective* regression relationships between the X- and the Y-space [18]. E.g. if already the t1-u1 relationships is (close to) linear, this is a certain reflection that a strong prediction model will be achieved; likewise, smaller non-linearities in the t1-u1 score plots are usually "ironed out" by inclusion of one or a few, *additional* PLS-components t2-u2, t3-u3 etc.
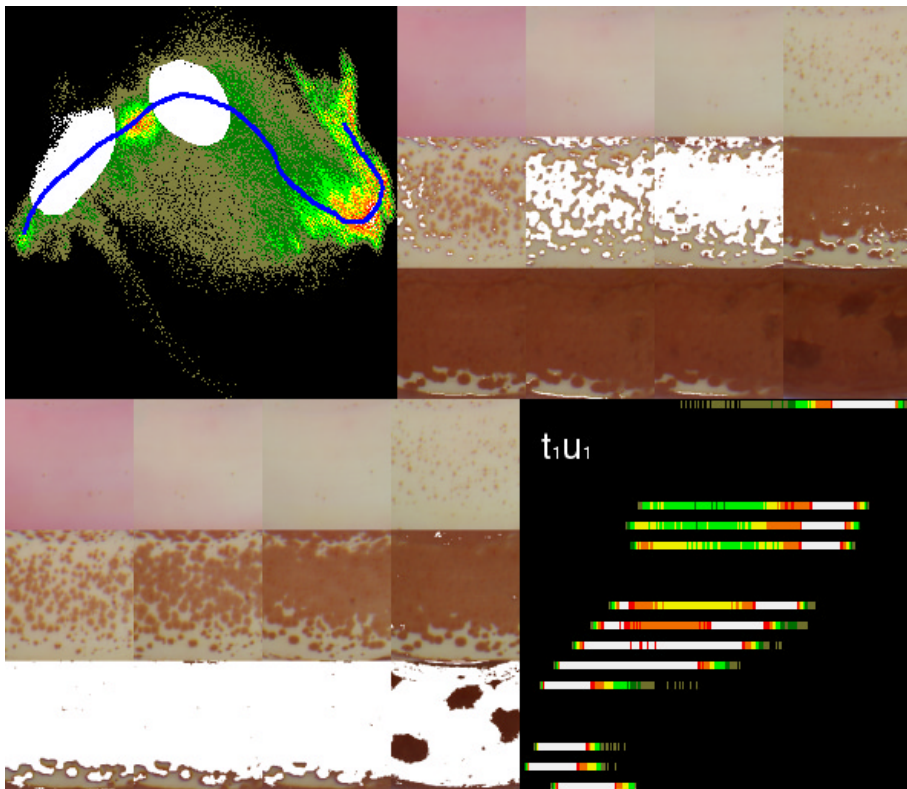

Figure 11. IPLS of the fruit aging process, in the IPLS-Y$_{grid}$ regression case. Upper left: t1-t2 score plot, with two sets of corresponding scene-space (upper right and lower left panels). Lower right: corresponding t1-u1 score plot. Note discrtesation along the u1-axis, corresponding to the Y-levels presented in figure 9.

For the present first presentation of the most used features in multivariate image regression, these few aspects of the general use of the t-u- plot will be enough to allow

appreciation of the way the IPLS-Y$_{grid}$-*modelling* works. Figures 11-13 represents salient central aspects of our work leading up to a complete *MIR strategy* [5,19].
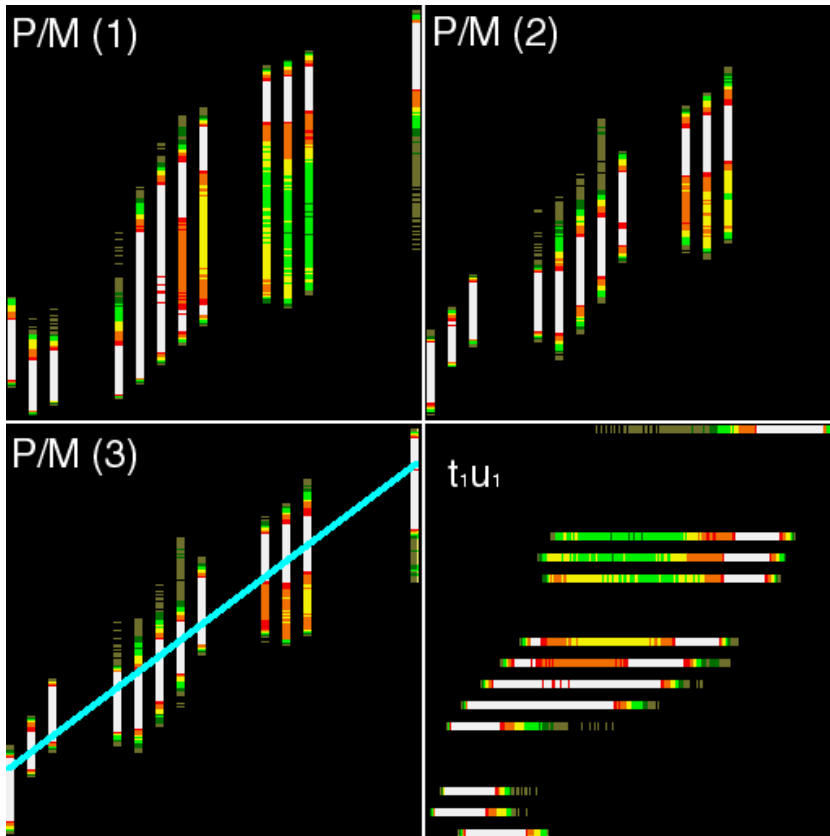

Figure 12. Complete predicted vs. measured (P/M) layout of the banana aging process IPLS-Ygrid-analysis. The standard P/M assessment plot is shown for 1,2 and 3 IPLS-components, while only the t1-u1 scoreplot is shown (lower right). Significant improvement of prediction precision using 3 components

For an assessment of the *modelling strength* of the IPLS-analysis, figures 11-13 will also suffice. From these X-Y relationships it is evident that a satisfactory model can be achieved using three IPLS-components. Observe e.g. how the P/M (*predicted* vs. *measured*) relationships improves quite considerably when adding the second - and third IPLS-components. From the t1-u1 relationships *alone* it was however already clear that this would *per force* result. We are also able to follow how one would go about identifying *outliers* etc. by using the appropriate t-u score plots, following [18]. In the specific present plots in Figure 11 we did actually not have reason to perform any outlier deletion, since none were found.
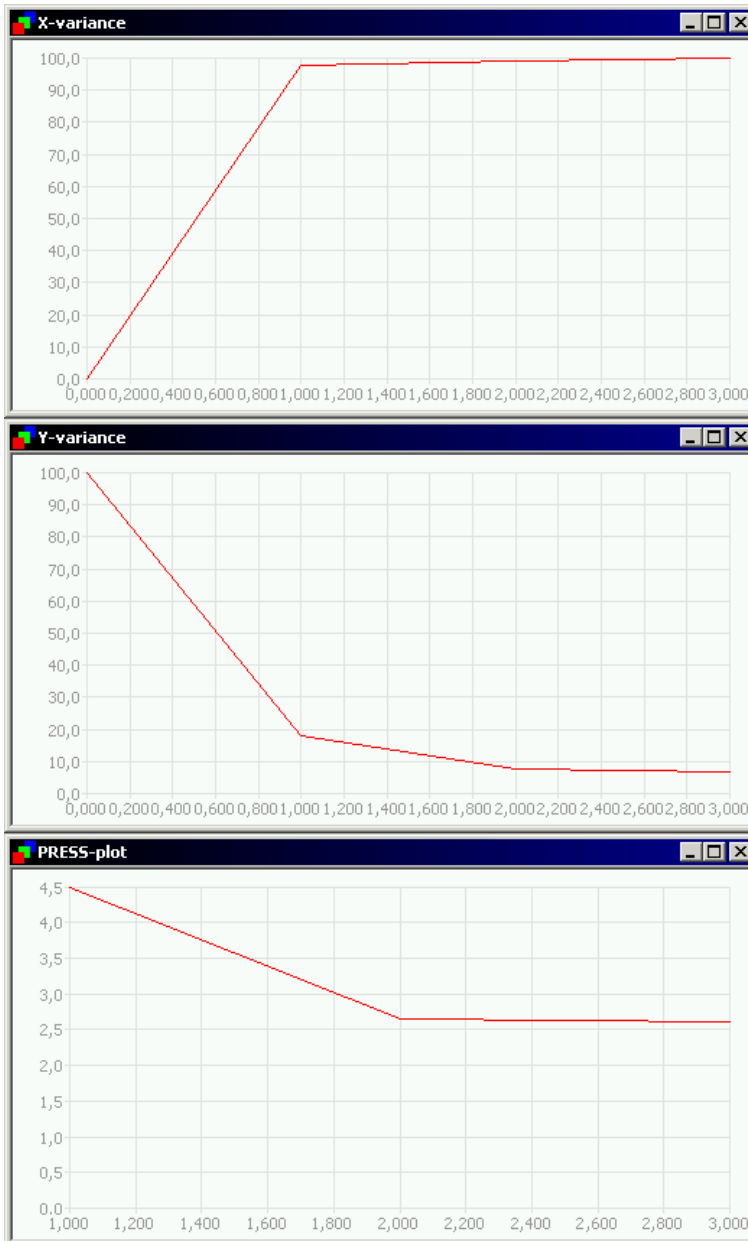
Figure 13. Calibrated X-variance (top) and Y-variance (middle) and validated PRESS (bottom) for banana aging case.

3.0 DISCUSSION AND CONCLUSIONS

The examples above represents our first presentation of a *simulation* of an <u>automated image-analysis monitoring system</u> in the guise of IPLS: MIR (and MIX), in which we focused on the general aspects of the IPLS-Y$_{discrim}$ and the IPLS$_{grid}$ *cases*.

The specific choices of illustrative food article systems is not in any way an absolute indication of the general applicability of this approach. What have been shown feasible for perishable fruit articles, and for on-line food product characterisation, is of course equally applicable to, say, cereals, bread, meat, fish - indeed the food and feed areas at large are potentially opened up for a similar approach, e.g. the berries -, beverages, - dairy sectors etc.

Continuing outside the human, and animal, food and feed areas, an *analogous* automated image monitoring approach can of course equally well be envisaged for quite different application areas, at first primarily within the general technological and industrial sectors - but perhaps even further removed. One common denominator could be any *multi-temporal* aspect, which would lend itself to an appropriately modified image recording and - analysis approach, *similar* to the one *illustrated* here, e.g. degradation studies: paints, coatings, corrosion inhabitation - industrial inspection in general i.a. Within the field of *remote sensing* there is also a plethora of similar multi-temporal objectives.

The on-line image monitoring example, while relatively simple in the crispbread case, also has many, much broader applications potentials within much of the *industrial inspection* realm, in which there is often a distinct need for automated image analytical monitoring.

For the present feasibility studies we are satisfied with the above results for both the *IPLS-Y$_{discrim}$* and the *IPLS-Y$_{grid}$* approaches. We have shown that the multivariate image regression approach (MIR) is now fully established. It bears in mind though, that there is always a series of critically important *specific* associated image-analytical problems, e.g. problem-specific illumination, shadows, reflections, non-constant object sizes i.a. - Much interesting work remains.

The present first foray into the possibilities of multivariate image regression has focussed on the ways-and-means of *modelling* (using bilinear IPLS) and *prediction*. What remains is the equally important aspect of multivariate calibration, *validation* (in the form of image-regression validation), which forms the subject-matter of the second

paper in this series, in which we also will make use of the third IPLS-regression case only identified here: Y_{total} [19].

References

1. K. Esbensen and P. Geladi; Chemometrics Intell. Lab. Syst. **7** (1989) pp. 67-86.

2. P. Geladi, and H. Grahn: Multivariate Image Analysis. John Wiley & Sons, Chichester, UK, 1996, p. 316.

3.   F. Lindgren, P. Geladi and S. Wold; J. Chemometrics, **7** (1993) 45-59

4. K. Esbensen, P. Geladi and H. Grahn; Chemometrics Intell. Lab. Syst**. 14** (1992) 67-86.

5. T.T. Lied, P. Geladi and K. Esbensen; J. Chemometrics **14** (2000) 585-598

6. N. Lamei, K.D. Hutchison, M.M. Crawford and N. Khazenie. Optical engineering **33** (1994): 1303-1313.

7. T. Yamazaki and D. Gingras. IEEE transactions on image processing **4** (1995) 1333-1339

8. J. R. Carr. Computers & Geosciences. **22** (1996), 849-865.

9. H. Martens and T. Næs: Multivariate Calibration. John Wiley & Sons, Chichester, UK, 1989, p. 419.

10. K. Esbensen, S. Wold and P. Geladi; J. Chemometrics, **3** (1988) pp. 33-48.

11. A.K. Smilde, J.A. Westerhuis and R. Boque; J. Chemometrics, **14** (2000), pp. 301-331.

12. R. Bro, Doctoral thesis. (1998): Multiway analysis in the food industry.

13. C. Anderson, and R. Bro (editors); J. Chemometrics **14** (2000): pp. 103-334.

14. A.K. Smilde, and H.A.L Kiers; J. Chemometrics **13** (1999) pp.31-48.

15. P. Geladi and K. Esbensen; J. Chemometrics **5** (1991) pp. 97-111.

16. J. P. Wold and K. Kvaal ; Appl. Spectrosc. **54**. (2000)

17. K. Esbensen, T.T. Lied, K. Lowell and G. Edwards. (Submitted for publication) Principles of Multivariate Image Analysis (MIA) in remote sensing, technology and industry.

18. K. Esbensen: Multivariate Analysis in Practice, 4th edition. (2000). CAMO ASA, Oslo, Norway.

19. T.T. Lied and K. Esbensen (Submitted for publication) Principles of MIR, Multivariate Image Regression -II: Cross validation- What you see is what you get.